Environmental Science Advances

ROYAL SOCIETY OF CHEMISTRY

PAPER

View Article Online
View Journal | View Issue

Cite this: *Environ. Sci.: Adv.*, 2025, **4**, 753

Revealing nighttime construction-related activities from a spatially distributed air quality monitoring network†

Jintao Gu,[a] Bo Yuan,[a] Shefford P. Baker,[b] Shaojun Zhang,[cd] Xiaomeng Wu,[c] Ye Wu[cd] and K. Max Zhang *[a]

In this study, through a novel network-based data-driven method, we reveal a likely unintended, nighttime-specific impact of construction activities on elevated coarse particulate matter (PM_c) concentrations in a metropolitan area. We analyzed the spatial and temporal patterns of coarse particulate matter (PM_c) levels in the urban part of a 165-node PM FEM monitoring network in Xi'an, China. We employed a novel technique called network analysis, which relies on data-driven, peer-to-peer comparisons within the monitoring network to identify regional events and local hotspots. Results revealed that the highest PM_c concentrations in the urban section of Xi'an occurred during late night and early morning. Aided by satellite-based aerial imagery and data mining of internet resources, we confirmed those peaks' strong association with construction-related sources. This observation is further supported by Land Use Regression (LUR) models, which demonstrate significant improvement in nighttime PMc prediction accuracy when they include a 'construction site' variable, an effect not observed during daytime. This finding underscores the significant impact of frequent nighttime construction activities and associated heavy-duty truck traffic ("dump trucks" responsible for transporting construction materials and wastes), which are likely unintentionally incentivized by both local policies and construction practices in many Chinese cities. Our work demonstrated the potential of utilizing air quality monitoring networks for construction-related environmental monitoring and enforcement. We also recommend that policymakers re-assess construction-related environmental and transportation policies by considering the trade-offs between air quality—the focus of our analysis—and other environmental and non-environmental considerations such as construction efficiency, traffic safety, noise, and waste management.

Received 3rd September 2024
Accepted 25th February 2025

DOI: 10.1039/d4va00334a

rsc.li/esadvances

Environmental significance

Evaluating the impact of construction-related emissions on air quality is very challenging, mainly due to (1) no centralized, publicly available reporting mechanisms to record the locations and construction progress and (2) construction-related emissions are highly localized. We report a novel approach called network analysis to capture the air quality impact of construction-related activities utilizing existing distributed air quality networks. We discovered a significant impact of frequent nighttime construction activities, unintentionally incentivized by local policies and construction practices in many Chinese cities. Our work demonstrated the potential of utilizing air monitoring networks for construction-related environmental monitoring and enforcement. We also recommend that policymakers re-assess construction-related environmental and transportation policies by considering the trade-offs among construction efficiency, air quality, noise, and waste management.

Introduction

Construction activities are a major source of particulate matter (PM) emissions, especially in urban areas.[1–7] For example, they are estimated to contribute 30% of PM_{10} emissions in London, UK, 17% of PM_{10} emissions in Germany, 42% of urban dust, a primary source for PM, in the Guanzhong Basin, China, and 26.4% of $PM_{2.5}$ emissions attributed to combined soil and construction dust in Tianjin city, China.[1–4] However, a comprehensive understanding of the impact of construction-related emissions on air quality is still very challenging due to several

[a]*Sibley School of Mechanical and Aerospace Engineering, Cornell University, Ithaca, NY, 14853, USA. E-mail: kz33@cornell.edu*

[b]*Department of Materials Science and Engineering, Cornell University, Bard Hall, Ithaca, New York, 14853, USA*

[c]*School of Environment, State Key Joint Laboratory of Environment Simulation and Pollution Control, Tsinghua University, Beijing 100084, China*

[d]*State Environmental Protection Key Laboratory of Sources and Control of Air Pollution Complex, Beijing 100084, China*

† Electronic supplementary information (ESI) available. See DOI: https://doi.org/10.1039/d4va00334a

factors. First, it is difficult to locate individual construction sites and track the status of each site. While the emissions from construction activities vary significantly depending on time duration, stage of construction, the machinery involved, road conditions, wind interactions, *etc.*,[2,5,6,8–11] there are no centralized, publicly available reporting mechanisms to record the locations and construction progress. As a result, construction sources are poorly represented in the emission inventories. For example, the National Emission Inventory (NEI) in the U.S. heavily relies on surrogate data and approximations to estimate fugitive PM emissions from construction sites at the county level.[12] The common method that the Chinese NEI guidebook adopts to estimate the dust emissions for individual construction sites also relies on a rough empirical formula.[13] Second, construction-related emissions are highly localized, with elevated concentrations confined within a few hundred meters.[10] It is worth noting that many construction-related activities, such as cutting, mixing, drilling, filling, loading/unloading, transporting, material stacking, and the carryout of mud and dirt, involve mechanical processes that generate coarse particles (PM_c).[6,8,11] As PM_c has a relatively short residence time, its spatial and temporal variations are expected to show great heterogeneity. Therefore, routine, sparsely sited air quality monitoring stations[14] are usually inadequate for directly capturing the impact of construction-related emissions.

Due to the challenges mentioned above, the research community and air quality regulators have mainly resorted to two types of approaches to understand the air quality impact of construction-related emissions. The first approach targets specific construction sites by setting up monitoring stations around those sites.[5,11,15–18] A study in London, UK, reported PM monitoring at 17 locations over 12 years near three construction sites in London. The study inferred the impact of construction activities by comparing data from upwind and downwind stations and analyzing working *versus* non-working hours.[10] The second approach relies on detailed chemical analysis of PM samples from a limited number of monitoring stations.[19–25] Researchers collected 244 diurnal PM samples over four months at a single location in Xi'an, China, for chemical analysis and inferred connections to construction dust based on the chemical composition and diurnal variations.[25] Both approaches have generated valuable knowledge to advance our understanding of construction-related emissions. However, neither approach is scalable to be widely implemented across a large region due to the high costs of dedicating air quality instruments to specific sites and conducting chemical analysis, respectively.

In this paper, we report a novel approach to capture the air quality impact of construction-related activities by taking advantage of existing distributed air quality networks. Deployed worldwide, distributed air quality monitoring networks, usually consisting of a large number of monitoring nodes across a large region, are designed to bridge the spatiotemporal gap of a sparse network for regulatory purposes. We introduce an innovative analytical method called network analysis, which serves as a screening tool to effectively process data from distributed air quality monitoring networks and generate insights about related emission sources. Specifically, the network analysis integrates two complementary techniques, *i.e.*, intra-/inter-ranking and time series clustering. Intra- and inter-ranking take advantage of peer-to-peer comparisons within the network to differentiate influences exerted by the regional events and local sources and identify the stations heavily influenced by local sources for further analysis. Instead of using mean diurnal patterns to analyze the diurnal properties of target pollutants, time series clustering captures day-to-day temporal-spatial differences, revealing representative diurnal patterns for further analysis.

Through our analysis, we captured the significant impact of nighttime construction activities, which has profound policy implications. The distributed air quality monitoring network we utilized to demonstrate our approach was deployed in Xi'an, China. Though many studies have focused on $PM_{2.5}$ and PM_{10} issues in Xi'an due to its severe pollution problems and large population, investigations on local construction sources in this city are rare.[26–40] Our analysis focuses on PM_c, as construction-related activities are a major source of PM_c compared to other sources, such as communing traffic and power generation. However, the general approach applies to other pollutants, *e.g.*, $PM_{2.5}$ and NO_2, which are commonly measured in distributed air quality networks.[41]

Materials and methods

Study domain and dataset

As a major metropolitan area in Northwest China, the municipality of Xi'an has a population of ~13 million, among which the urban population accounts for around 9 million.[42,43] Our study utilized data from a PM monitoring network in Xi'an, shown in Fig. 1, consisting of 165 Beta attenuation monitoring (BAM)-based monitoring stations.[44] BAM employs the absorption of beta radiation by solid particles extracted from air flow to detect PM_{10} and $PM_{2.5}$ and is a Federal Equivalent Method (FEM) approved by the U.S. Environmental Protection Agency (EPA).[45] Each station was designed with an ID (*e.g.*, 1201C) using

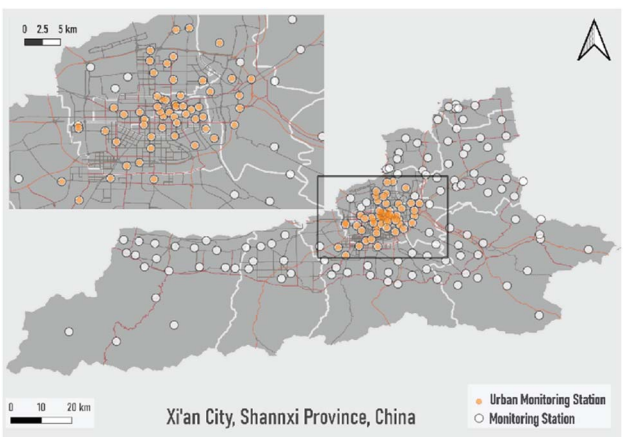

Fig. 1 The air quality monitoring network in Xi'an city. Monitoring stations located in the main urban area are defined as urban monitoring stations and are selected as targets (orange ones).

a 4-digit number followed by the letter "C", which stands for "Community monitoring". Hourly data were collected in April and May 2020, and PM_c concentrations were then derived from PM_{10} and $PM_{2.5}$. Xi'an's densely populated urban areas were targeted for our research due to its high population density, high density of monitoring stations (56 monitoring stations marked in the orange color in Fig. 1), and relatively higher PM_c concentrations than other regions. For information on the statistical analysis of the data and data preprocessing, see Table S1 in the ESI.†

Network analysis

The main goal of our network analysis is to provide insights on both areas and emission sources of interest within the monitoring network using peer-to-peer comparison. The three main techniques, *i.e.*, intra- and inter-ranking, time series clustering, and data mining, are described as follows.

Intra-ranking and inter-ranking: identify the areas and periods of interest. First, an intra-ranking system was created to identify the potential network-wide phenomena. The daily averaged PM_c concentrations recorded at the same monitoring station ("intra") were ranked to identify periods when a pollution episode happened across the urban network regardless of specific locations. Since our main interests are local emission sources, we excluded the identified regional event days for further steps. Next, an inter-ranking system was created to identify urban stations potentially influenced by recurring local emission sources and related events. We ranked the daily averaged PM_c concentrations among all the urban monitoring stations ("inter") after excluding identified periods with regional events from the intra-ranking system. Those stations consistently ranked among the highest were called hotspots and were used for further analysis.

Time series clustering: extract diurnal patterns associated with hotspot sites. After identifying the stations of interest (hotspots) and periods of interest (days less influenced by regional events), we applied the time series clustering method to all individual diurnal curves. Diurnal curves with incomplete data were excluded, and 2041 diurnal curves were conserved. The main objective for the time series clustering is to compare the diurnal patterns between the hotspot sites and the rest of the urban sites. We took several steps to achieve this objective. The elbow method[46] was utilized to find the appropriate number (*i.e.*, 30, shown in Fig. S1†) of clusters, and the *K*-means algorithm[47–49] was adopted for time series clustering. The diurnal patterns shared by a large number of non-hotspot sites and by hotspot sites, respectively, were selected and analyzed to pinpoint any unique patterns for the hotspot sites. More information on the algorithm and data processing is shown in Section S2.†

Data mining: generate emission-related features. Understanding the drivers of the unique diurnal patterns associated with hotspot sites is valuable in informing effective mitigation strategies. We collected information from various data sources to generate features related to potential emission sources. Our efforts focused on construction-related activities and traffic as they are the main contributors to local PMc emissions (see Section S3†).[50–53] The data sources for our investigation included emission inventories, GIS-based data layers from Open Street Map (OSM) and governmental agencies, satellite imagery from Google and Baidu, online discussion forums, governmental and real estate developer websites, *etc.* In addition, hourly traffic counts were sampled from the selected period on weekdays and weekends for 77 149 road sections in Xi'an with detailed information shown in Table S3 and Fig. S2.†

Gathering accurate construction site information has been a challenge for air quality studies. To ensure the quality of our analysis, we screened all the monitoring sites and verified the presence of construction-related activities during the sampling period through multiple independent sources. We used Site 1201C to explain the verification process, described as follows.

The initial screening process using Google Satellite imagery identified tower cranes and scaffoldings near Site 1201C, as shown in Fig. 2(a). Similar construction activities were shown in another online service, Baidu Satellite Fig. 2(b). After acquiring the Chinese name of this potential construction site from Baidu Satellite, we conducted extensive online searches based on the name, revealing additional information to confirm the construction activities during the sampling period. As presented in Fig. 2(c), residents filed complaints about the nighttime noise disturbance through online forums administrated by the local government in September 2020. They received an official reply stating that the main body of the building was being constructed and that the local environmental protection agency approved the nighttime construction. The local environmental protection department replied in December 2021 that construction materials had to be transported at night due to the traffic restriction, stating the permitted construction period was between June 2019 and January 2022. Thus, we were able to confirm an active construction site under the main body construction stage with overnight construction activities existing around station 1201C during the target period.

Following a similar process, nineteen urban stations were identified with active construction sites nearby, and the terms "Construction Station" and "Non-Construction Station" were used to refer to the monitoring station with/without an active construction site nearby.

Results and discussion

Intra-ranking and inter-ranking system analysis

Fig. 3(a) and S3† illustrate network-wide (*i.e.*, regardless of locations) episodes from the intra-ranking of daily average PM_c concentrations. Notably, elevated PM_c concentrations across the network during May 17th–18th, later confirmed as a dust storm event, were due to natural dust transport outside the city under strong wind conditions. Regional events like rain could lead to a low PM_c concentration across the network, evident in the case of April 18th–19th. After a rain, all the urban stations dropped to a relatively low PM_c concentration level compared with themselves in the selected two months, which form a deep blue (ranking < 20%) area in Fig. 3(a). After excluding fifteen days influenced by regional events identified by the intra-

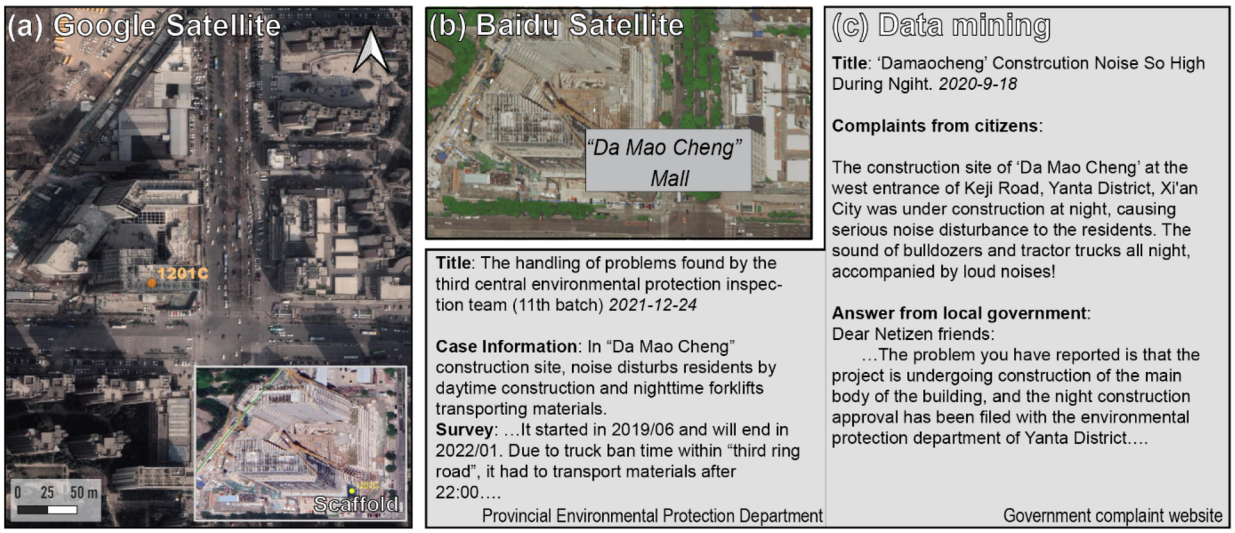

Fig. 2 Verification of construction site: an example for monitoring station 1201C. Process: (a) locate a potential construction site around 1201C using Google Satellite. (b) Access the construction's name using Baidu Satellite. (c) Conduct data mining on the internet. In this case, construction was active during the target period with overnight construction activities, leading to many complaints from nearby residents.

ranking system analysis and other datasets (with more description in Fig. S3†), we performed the inter-ranking to select the monitoring stations that consistently ranked high in concentrations in the network. Stations sorted by high-ranking (*i.e.*, top 10) days fraction (defined as the number of high-ranking days/the number of total days with records) are shown in Fig. 3(b). Thirteen stations with significantly more high-ranking days (13th is 15 days while 14th is 12 days) were designated as hotspots in this study.

Time series clustering

The clustering results for all thirty clusters are visualized in Fig. S4,† and their temporal-spatial distributions and sizes are shown in Fig. S5 and S6,† respectively. Nine representative clusters, with their mean diurnal profiles shown in Fig. 4, were

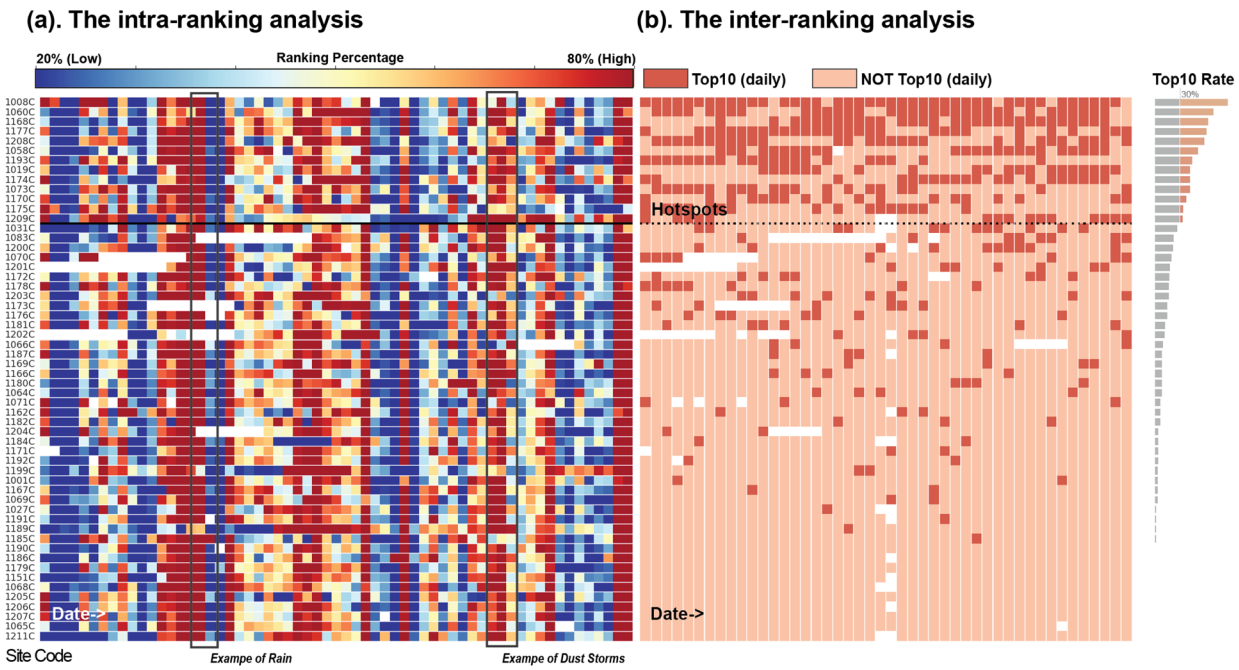

Fig. 3 Intra-ranking and inter-ranking system analysis results: (a) Heatmap of intra-ranking system results. Episodes, regardless of locations, could be observed, indicating the existence of regional events such as rain and dust storms shown in two cases.[69] Days with regional event records are excluded for further analysis. (b) The color of one block in the heatmap represents whether a monitoring station (y-axis) was top 10 in the inter-ranking system within a single day (x-axis). Thirteen monitoring stations with consistently high PM_c concentrations are identified as hotspots for further analysis.

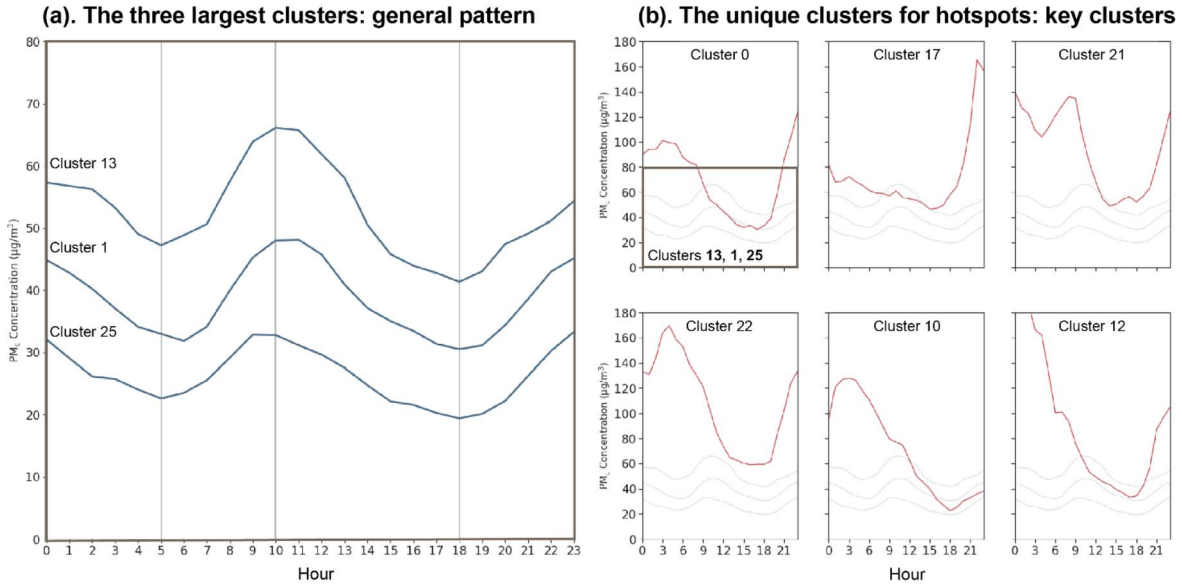

Fig. 4 (a) The general patterns identified by the largest clusters (1, 13, and 25) showed two peaks at night and morning. (b) Compared to the general patterns, all unique clusters for the hotspots (called key clusters) showed much elevated concentrations during the night or early morning, and most of them did not show a prominent morning peak, indicating the potential existence of a strong local driver. The lightly shaded lines in (b) are the same as the solid lines in (a) for comparison purposes.

selected for the subsequent discussions. Three clusters of the largest size (1, 13, 25), shown in Fig. 4(a), depicted the general patterns for most of the monitoring stations: two peaks (around midnight, 23:00–0:00, and in the morning, 8:00–10:00) and two valleys (around early morning, 4:00–5:00 and early evening around 18:00). This type of diurnal patterns with both morning and nighttime peaks was also found in other clusters with relatively larger sizes (more analysis presented in Section S3, Fig. S7–S11, and Table S5†). This general diurnal pattern is likely governed by mixing height and traffic. The traffic generates non-exhaust particle emissions (mainly about PM_c) from the wearing down of brakes, clutches, tires, and road surfaces, as well as by the suspension of road dust,[54] and the mixing height influences the PM_c concentration level by affecting its dispersion rate.[55–57] As Fig. S7† shows, the data matches the explanation well: The morning peak is dominated by high traffic counts; the early evening valley is caused by a large mixing height; the midnight peak is a result of a low mixing height; and the early morning valley is influenced by low traffic counts.

The other six clusters, shown in Fig. 4(b), represented the unique patterns for hotspots with a higher than 50% relative count (defined as the number of diurnal curves from hotspots divided by the total number of diurnal curves in a cluster; for example, cluster 7's relative count is 45%). These six clusters were referred to as key clusters, where 72% of the total diurnal curves inside are from hotspots. Compared to the general diurnal pattern, the key clusters not only generally had much higher PM_c concentrations than the other clusters but also showed significantly elevated PM_c peaks during early morning or nighttime and the absence of the morning peak around 10:00. The patterns of key clusters cannot be explained by either the typical traffic or mixing height trends and require further investigations.

PM_c hotspots are linked to nighttime construction-related activities

Further analysis linked the unique patterns associated with hotspots (*i.e.*, the patterns of key clusters shown in Fig. 4(b)) to the nighttime construction site activities. First, more construction stations (8 out of 19) were identified as hotspots

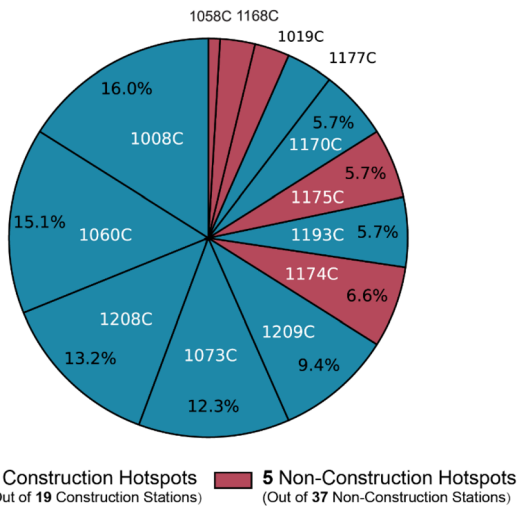

Fig. 5 The contribution of individual hotspots to diurnal curves in hotspots clustered into key clusters. Construction hotspots are the main contributor (~81%) to these clusters, indicating construction activities may lead to the abnormally high concentration in the night and early morning of these clusters.

compared to non-construction stations (5 out of 37). Second, as shown in Fig. 5, when looking at the diurnal curves in hotspots clustered into key clusters, ~81% of them are contributed by construction hotspots. Both of them indicated the potential linkage.

The relationship between nighttime construction site activities and unique patterns was further verified and evaluated by examining all the urban stations, including both hotspots and non-hotspots. The PM_c hourly records ($N = 55\,180$) were divided into two categories based on the time of day – daytime (7:00 to 19:00) and nighttime (20:00 to 6:00). Following this, the Complementary Cumulative Distribution Function (CCDF) for these records from both construction and non-construction stations were individually graphed for each time period, as illustrated in Fig. 6(a) and (b). Construction stations displayed markedly higher PM_c concentrations and more extreme values (*i.e.*, above 100 and 150 μg m^{-3}) than non-construction stations, with no such trend observed during the daytime. Specifically, at nighttime, construction stations had a 26.1% higher average PM_c concentration (66.5 μg m^{-3} *vs.* 52.7 μg m^{-3}). Furthermore, construction stations were almost twice more likely to register readings above 100 μg m^{-3} (18.0% *vs.* 8.1%) and three times more likely for 150 μg m^{-3} (4.5% *vs.* 1.4%) than the non-construction stations. Additionally, as shown in the embedded plots in Fig. 6(a) and (b), construction stations had higher station-individual mean values during nighttime (raw data and additional analysis on other individual statistics are in Fig. S16, Tables S7, S8, and Section S7,† $N = 55$), with statistically significant differences (CI = 99%) by the Mann–Whitney U test.[58] In contrast, during the daytime, there was no significant difference between the two groups ($p = 0.13$), verifying that construction stations differ from non-construction stations in PM_c concentration mainly during nighttime rather than daytime.

Impact of construction sites on nighttime PM_c levels in LUR models

Though differences in PM_c nighttime levels between non-construction stations and construction were observed, we aimed to confirm that these differences were primarily due to active construction sites rather than other factors. A potential way here is to designate "Construction Site" as a binary variable and assess its impact by integrating it with other spatial predictor variables related to pollution levels into statistical models. We selected nearly 300 spatial variables, covering land use area, road length, and Points of Interest (POIs), such as bus stops, traffic volume, and population density, across different buffer radii (if applicable), as detailed in Table S8.†

We utilized Land Use Regression (LUR) models to predict average PM_c levels at stations during both daytime and nighttime. The modeling was also performed with and without the "Construction Site" variable in the final model, resulting in four distinct models (Table 1). For each model, pre-selection was conducted to avoid multicollinearity, followed by an exhaustive search subset selection with maximum adjusted R^2 in Ordinary Least Squares (OLS) regression, adhering to a rule-of-thumb of a maximum of one predictor per ten samples, capped at five.[59,60] Additionally, all predictors must demonstrate statistical significance with p-values less than 0.1.[59] Model performance was evaluated using R^2, and root mean squared error (RMSE) metrics, derived from Leave-One-Out Cross-Validation (LOOCV) and 100-time 5-fold Cross-Validation (CV).

Table 1 reveals that the inclusion of the "Construction Site" variable enhances nighttime models; its absence resulted in an LOOCV R^2 of 0.46 and an RMSE of 10.25 μg m^{-3}, while its inclusion (with an OLS coefficient of 8.88) increased the LOOCV R^2 to 0.54 and reduced the RMSE to 9.45 μg m^{-3}. This improvement is also mirrored in the 100-times 5-fold CV results, showing significantly improved R^2 (0.33 to 0.43, N =

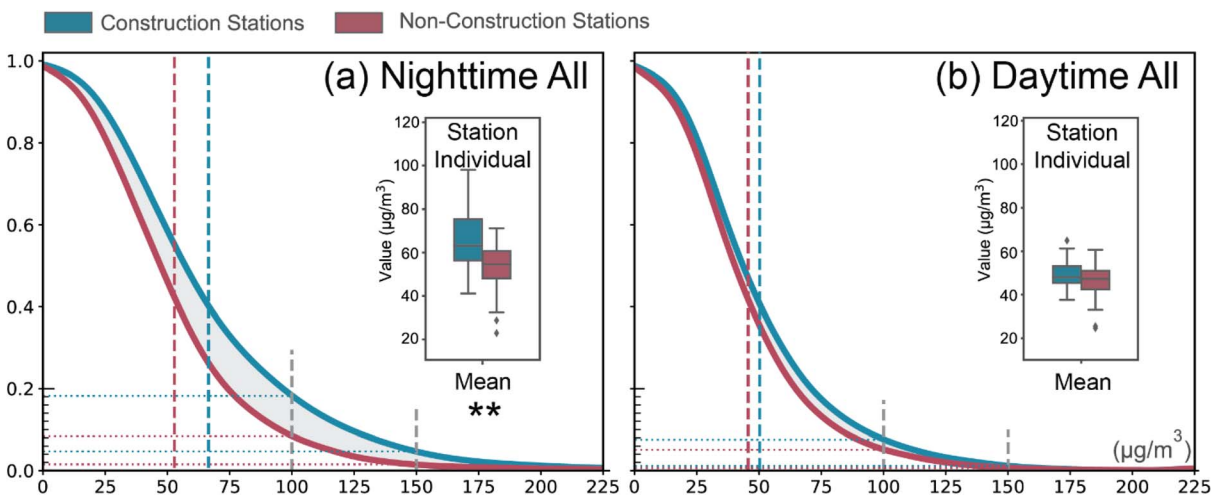

Fig. 6 (Main) The complementary cumulative distribution function (CCDF) for hourly PM_c readings of construction stations and non-construction stations during (a) nighttime (20:00 to 6:00) and (b) daytime (7:00 to 19:00). (Inset) The station-individual mean values for construction stations and non-construction stations during (a) nighttime and (b) daytime (**: p-value ≤ 0.01). Significant differences between construction and non-construction stations were mainly found at nighttime, indicating that the impact of construction activities on PM_c has a temporal attribute of night.

Table 1 Performance metrics of four Land Use Regression (LUR) models for estimating station-mean PM_c concentration levels (μg m^{-3}) during daytime and nighttime across 55 instances, considering the inclusion and exclusion of the 'Construction Site' feature in final model. 304 other spatial features were considered. Notably, the inclusion of 'Construction Site' boosts model performance during nighttime, an effect not mirrored in daytime

	"Construction Site" in final model	Adj. R^2	LOOCV R^2	LOOCV RMSE (μg m^{-3})	100-time 5-fold CV R^2		RMSE (μg m^{-3})	
					Mean	Std	Mean	Std
Nighttime	With	0.61	0.54	9.45	0.43	0.40	9.63	2.40
	Without	0.56	0.46	10.25	0.33	0.53	10.35	2.40
Daytime	With	0.42	0.33	6.59	0.26	0.40	6.54	1.45
	Without	0.57	0.52	5.60	0.43	0.30	5.70	1.03

500) and RMSE values (10.35 μg m^{-3} to 9.63 μg m^{-3}, $N = 500$) with lower or similar variation. In contrast, during daytime, the addition of this variable (coefficient: 3.21 in the OLS model) not only failed to improve, but also worsened performance, underscoring its limited impact on daytime PM_c levels. These findings indicate that active construction sites primarily have a strong impact on PM_c levels at night rather than during the day, and other common spatial pollution indicators do not mirror this relationship. For details on our variable selection, LUR model settings, and results, see Section S8 and Table S9.†

Although the performance of our PM_c models is not as high as seen in some $PM_{2.5}$ and PM_{10} LUR modeling studies,[61] it is still considered acceptable for variable verification in PM_c modeling. This is because PM_c models generally exhibit a much worse performance than $PM_{2.5}$ and PM_{10} models, with LOOCV R^2 values differing by 0.1 to 0.3 and sometimes as low as 0.22 in those rare studies that contain PM_c LUR modeling.[62–64] An improvement of 0.1 on 100-time 5-fold CV R^2 is considered significant due to the smaller baseline (0.33), more stable performance, and the fact that our "without nighttime" model already encompasses the most common LUR features.

Although common factors were considered in the LUR model to confirm that nighttime PM_c heterogeneity persists between construction and non-construction stations after accounting for these variables, some station-specific factors were not included in this study due to data availability and methodological constraints. Factors such as urban canyons and their interactions with microclimatic variables [65,66] are important for a deeper understanding of PM_c concentration patterns and should be considered in future analyses if condition permits.

Nighttime PM_c hotspots as an unintended consequence of environmental policies

Our network analysis and further verification by LUR models attribute the nighttime peaks in PM_c concentrations to construction-related activities. A further review of the literature on construction-related emissions and environmental policies suggested the critical role of heavy-duty trucks responsible for transporting construction materials such as soil, sand, and waste, also known as "dump trucks". According to an interview-based study in China, the transportation of soil is recognized as the largest contributor to construction dust.[67] PM emissions (mainly PM_c) from construction activities, mainly from earthmoving, truck loading/unloading, the transportation of mud and dirt, and the resuspension of dust from unpaved roads,[6] are all directly related to dump truck traffic.[68]

It is important to point out that the regulations on dump trucks are often developed separately from those imposed on other heavy-duty trucks (such as freight vehicles) in China. Many Chinese cities, including Xi'an, have adopted a daytime ban or designated nighttime as the primary operating window for dump trucks, originally developed for traffic safety and environmental considerations (see Section S9.1 and Table S10†). Between 2011 and 2019, Xi'an permitted dump truck operations only from 22:00 to 6:30. Since 2019, an additional operating window from 10:00–16:00 has been introduced to address the growing construction waste problem. However, several factors unintentionally incentivized construction contractors to conduct a majority of the most emission–intensive activities (such as excavation and subsequent dump truck operations) during nighttime. For example, even though stringent dust control regulations exist for dump trucks (such as load limits, dust covers, and body wash), enforcing these environmental measures is often lax during nighttime. In addition, the few traffic congestions and the lack of enforcement of traffic regulations are also favorable factors for nighttime dump truck operations. Essentially, the nighttime hours have become a "convenient" time window for dump trucks to be non-compliant with both air quality and traffic regulations from a purely cost-reduction perspective. The consequences include elevated air pollution and noise pollution levels, as well as many reported nighttime traffic accidents resulting in injuries and fatalities (for related news coverage, see Section S9.2).

Our study indicates that the observed nighttime peaks in PM_c concentration are one of the unintended consequences of environmental and traffic policies on dump trucks. The implied policy interventions include (1) strengthening the enforcement of related regulations during nighttime and (2) examining the costs and benefits of controlling nighttime dump truck operations. Transitioning to a policy that limits nighttime dump truck operations is worthy of debate since daytime meteorological conditions (such as greater mixing layer heights) are generally less conducive to high PM concentrations, and compliance among dump truck operators is likely to be higher. To the best of our knowledge, the City of Changsha in Hunan Province is the only municipality in China that has implemented a nighttime restriction on dump truck operations.

Starting from January 2020, dump trucks are not allowed to operate between midnight and 9:30, and special permits are required to operate dump trucks from 22:00 to midnight. Benefits, including controlling fugitive dust, reducing nighttime traffic noise, and preventing traffic violations, were cited by policymakers as the main rationales for the nighttime restriction (see Section S9.3†), which aligns with our findings. We advocate for a comprehensive analysis including construction efficiency, air pollution, noise pollution, waste management, and road safety to examine the complex trade-offs in different policy options related to dump trucks.

Conclusions

Our network analysis offers a practical screening tool for regulators to efficiently analyze a large amount of air quality data collected from distributed sensor networks, identify hotspots, and link them to potential emission sources. We utilized construction sites to demonstrate the benefits of the network analysis approach. Our findings revealed that construction-related emissions significantly impact PM_c levels during the nighttime but not during the daytime, and we confirmed this observation by developing LUR models considering other spatial variables. Existing dump-truck related environmental policies could explain this day–night discrepancy. A limitation of our study is the lack of quantitative analysis of station heterogeneity regarding some specific spatial and spatio-temporal factors, such as urban canyons, microclimates, and background concentrations, which are important for deeper insights. Future research may involve considering these factors through further data collection, detailed data compilation from diverse construction sites at various stages and proximal reference monitoring stations for comprehensive impact assessment of construction dump trucks and other activities.

Data availability

The raw data from the community monitoring network are not provided due to the legal confidentiality requirements. Detailed statistics supporting this article are included in the ESI.†

Author contributions

Jintao Gu: conceptualization, methodology, investigation, writing-original draft, reviewing and editing. Bo Yuan: investigation, writing-reviewing and editing. Shefford Baker: writing, reviewing and editing. Shaojun Zhang: methodology, investigation, writing-reviewing and editing. Xiaomeng Wu: data curation. Ye Wu: data curation, methodology. K. Max Zhang: conceptualization, methodology, investigation, writing-reviewing and editing, supervision and funding acquisition.

Conflicts of interest

There are no conflicts to declare.

Acknowledgements

The authors would like to acknowledge the support from the Cornell China Center and valuable discussions with Dr Jinhua Zhao, Dr Jiajun Gu, Henry Williams at Cornell University, and Dr Junshi Xu at The University of Hong Kong.

Notes and references

1 J. Gao, K. Wang, Y. Wang, S. Liu, C. Zhu, J. Hao, H. Liu, S. Hua and H. Tian, *Environ. Pollut.*, 2018, **233**, 714–724.
2 P. Faber, F. Drewnick and S. Borrmann, *Atmos. Environ.*, 2015, **122**, 662–671.
3 *London Atmospheric Emissions Inventory (LAEI)*, 2019.
4 N. Li, X. Long, X. Tie, J. Cao, R. Huang, R. Zhang, T. Feng, S. Liu and G. Li, *Sci. Total Environ.*, 2016, **541**, 1614–1624.
5 X. Fang, R. Chang, Y. Zhang, J. Zuo, Y. Zou and Y. Han, *J. Build. Eng.*, 2024, **86**, 108708.
6 J. S. Kinsey and C. Cowherd, *J. Air Waste Manage. Assoc.*, 2005, **55**, 772–783.
7 Y. Z. Tian, G. L. Shi, Y. Q. Huang-Fu, D. L. Song, J. Y. Liu, L. D. Zhou and Y. C. Feng, *Sci. Total Environ.*, 2016, **557–558**, 697–704.
8 F. Azarmi, P. Kumar and M. Mulheron, *J. Hazard. Mater.*, 2014, **279**, 268–279.
9 H. Yan, Q. Li, K. Feng and L. Zhang, *Environ. Sci. Pollut. Res.*, 2023, **30**, 62716–62732.
10 F. Azarmi, P. Kumar, D. Marsh and G. Fuller, *Environ. Sci.:Processes Impacts*, 2016, **18**, 208–221.
11 D. Cheriyan, K. Khamraev and J. ho Choi, *Sustain. Cities Soc.*, 2021, **72**, 103016.
12 2020 National Emissions Inventory (NEI) Data, US EPA, **https://www.epa.gov/air-emissions-inventories/2020-national-emissions-inventory-nei-data#doc**, accessed 11 February 2023.
13 *Technical Guidelines for the Compilation of Dust Source Particulate Matter Emission*, 2014, pp. , pp. 70–86.
14 C. A. Keet, J. P. Keller and R. D. Peng, *Am. J. Respir. Crit. Care Med.*, 2018, **197**, 737–746.
15 H. Yan, G. Ding, K. Feng, L. Zhang, H. Li, Y. Wang and T. Wu, *J. Cleaner Prod.*, 2020, **275**, 122767.
16 S. Ahmed and I. Arocho, *J. Build. Eng.*, 2019, **22**, 281–294.
17 Q. Luo, L. Huang, Y. Liu, X. Xue, F. Zhou and J. Hua, *Sustainability*, 2021, **13**, 1–21.
18 W. Jaafar, J. Xu, E. Farrar, C. H. Jeong, A. Ganji, G. Evans and M. Hatzopoulou, *Build. Environ.*, 2024, **254**, 111363.
19 P. Kassomenos, S. Vardoulakis, A. Chaloulakou, G. Grivas, R. Borge and J. Lumbreras, *Atmos. Environ.*, 2012, **54**, 337–347.
20 P. Kumar, P. K. Hopke, S. Raja, G. Casuccio, T. L. Lersch and R. R. West, *Atmos. Environ.*, 2012, **46**, 449–459.
21 K. Cheung, N. Daher, W. Kam, M. M. Shafer, Z. Ning, J. J. Schauer and C. Sioutas, *Atmos. Environ.*, 2011, **45**, 2651–2662.
22 T. A. Pakkanen, K. Loukkola, C. H. Korhonen, M. Aurela, T. Mäkelä, R. E. Hillamo, P. Aarnio, T. Koskentalo, A. Kousa and W. Maenhaut, *Atmos. Environ.*, 2001, **35**, 5381–5391.

23 W. C. Malm, M. L. Pitchford, C. McDade and L. L. Ashbaugh, *Atmos. Environ.*, 2007, **41**, 2225–2239.
24 S. Choung, J. Oh, W. S. Han, C. M. Chon, Y. Kwon, D. Y. Kim and W. Shin, *Sci. Total Environ.*, 2016, **541**, 1132–1138.
25 D. Ainur, Q. Chen, T. Sha, M. Zarak, Z. Dong, W. Guo, Z. Zhang, K. Dina and T. An, *Environ. Sci. Technol.*, 2023, **57**, 9252–9265.
26 G. H. Wang, C. L. Cheng, Y. Huang, J. Tao, Y. Q. Ren, F. Wu, J. J. Meng, J. J. Li, Y. T. Cheng, J. J. Cao, S. X. Liu, T. Zhang, R. Zhang and Y. B. Chen, *Atmos. Chem. Phys.*, 2014, **14**, 11571–11585.
27 M. Wang, Z. Zhang, Q. Yuan, X. Li, S. Han, Y. Lam, L. Cui, Y. Huang, J. Cao and S. cheng Lee, *Sci. Total Environ.*, 2022, **841**, DOI: **10.1016/j.scitotenv.2022.156740**.
28 Z. Wang, R. Wang, J. Wang, Y. Wang, N. McPherson Donahue, R. Tang, Z. Dong, X. Li, L. Wang, Y. Han and J. Cao, *Environ. Res.*, 2022, **212**(Part C), DOI: **10.1016/j.envres.2022.113388**.
29 P. Wang, J. ji Cao, Z. xing Shen, Y. ming Han, S. cheng Lee, Y. Huang, C. shu Zhu, Q. yuan Wang, H. mei Xu and R. jin Huang, *Sci. Total Environ.*, 2015, **508**, 477–487.
30 H. Xu, J. Cao, J. C. Chow, R. J. Huang, Z. Shen, L. W. A. Chen, K. F. Ho and J. G. Watson, *Sci. Total Environ.*, 2016, **545–546**, 546–555.
31 X. Niu, J. Cao, Z. Shen, S. S. H. Ho, X. Tie, S. Zhao, H. Xu, T. Zhang and R. Huang, *Atmos. Environ.*, 2016, **147**, 458–469.
32 D. Wang, J. Hu, Y. Xu, D. Lv, X. Xie, M. Kleeman, J. Xing, H. Zhang and Q. Ying, *Atmos. Environ.*, 2014, **97**, 182–194.
33 Z. Shen, J. Cao, R. Arimoto, Y. Han, C. Zhu, J. Tian and S. Liu, *Aerosol Sci. Technol.*, 2010, **44**, 461–472.
34 W. Huang, J. Cao, Y. Tao, L. Dai, S. E. Lu, B. Hou, Z. Wang and T. Zhu, *Am. J. Epidemiol.*, 2012, **175**, 556–566.
35 X. Liu, Y. Hui, Z. Y. Yin, Z. Wang, X. Xie and J. Fang, *Theor. Appl. Climatol.*, 2016, **125**, 321–335.
36 Y. Chen, J. Cao, R. Huang, F. Yang, Q. Wang and Y. Wang, *Sci. Total Environ.*, 2016, **573**, 937–945.
37 J. J. Cao, Q. Y. Wang, J. C. Chow, J. G. Watson, X. X. Tie, Z. X. Shen, P. Wang and Z. S. An, *Atmos. Environ.*, 2012, **59**, 559–566.
38 Q. Dai, X. Bi, B. Liu, L. Li, J. Ding, W. Song, S. Bi, B. C. Schulze, C. Song, J. Wu, Y. Zhang, Y. Feng and P. K. Hopke, *Environ. Pollut.*, 2018, **240**, 155–166.
39 M. Elser, R. J. Huang, R. Wolf, J. G. Slowik, Q. Wang, F. Canonaco, G. Li, C. Bozzetti, K. R. Daellenbach, Y. Huang, R. Zhang, Z. Li, J. Cao, U. Baltensperger, I. El-Haddad and P. André, *Atmos. Chem. Phys.*, 2016, **16**, 3207–3225.
40 L. Han, J. Zhao, Y. Gao, Z. Gu, K. Xin and J. Zhang, *Sustain. Cities Soc.*, 2020, **61**, 102329.
41 X. Zheng, S. Zhang, Y. Wu, K. M. Zhang, X. Wu, Z. Li and J. Hao, *Environ. Pollut.*, 2017, **231**, 348–356.
42 Xi'an, **http://en.shaanxi.gov.cn/as/cities/201705/t20170505_1595150.html**, accessed 28 July 2022.
43 Economic and social development statistical chart: Basic population situation of super-large and mega-cities in the seventh national census – Qiushi.com, **http://www.qstheory.cn/dukan/qs/2021-09/16/c_1127863567.htm**, accessed 28 July 2022.
44 E. S. Macias and R. B. Husar, *Environ. Sci. Technol.*, 1976, **10**, 904–907.
45 eCFR, 40 CFR Part 53 – Ambient Air Monitoring Reference and Equivalent Methods, **https://www.ecfr.gov/current/title-40/chapter-I/subchapter-C/part-53**, accessed 11 July 2022.
46 R. L. Thorndike, *Psychom*, 1953, **184**(18), 267–276.
47 D. Arthur and S. Vassilvitskii, *Proc. Annu. ACM-SIAM Symp. Discret. Algorithms*, 2007, pp. 1027–1035.
48 R. Xu and D. C. Wunsch, *Clustering*, 2009, 63–110.
49 H. Teichgraeber and A. R. Brandt, *Appl. Energy*, 2019, **239**, 1283–1293.
50 D. Chen, S. Cheng, Y. Zhou, X. Guo, S. Fan and H. Wang, *Environ. Eng. Sci.*, 2010, **27**, 825–834, DOI: **10.1089/ees.2009.0122**.
51 Z. Zhou, Q. Tan, Y. Deng, K. Wu, X. Yang and X. Zhou, *J. Atmos. Chem.*, 2019, **76**, 21–58.
52 V. Singh, A. Biswal, A. P. Kesarkar, S. Mor and K. Ravindra, *Sci. Total Environ.*, 2020, **699**, 134273.
53 T. Li, W. Dong, Q. Dai, Y. Feng, X. Bi, Y. Zhang and J. Wu, *Sci. Total Environ.*, 2021, **798**, 149114.
54 OECD, *Non-exhaust Particulate Emissions from Road Transport*, DOI: **10.1787/4A4DC6CA-EN**.
55 K. Schäfer, S. Emeis, H. Hoffmann and C. Jahn, *Meteorol. Z.*, 2006, **15**, 647–658.
56 P. Wagner and K. Schäfer, *Urban Clim.*, 2017, **22**, 64–79.
57 J. Rost, T. Holst, E. Sähn, M. Klingner, K. Anke, D. Ahrens and H. Mayer, *Int. J. Environ. Pollut.*, 2009, **36**, 3–18.
58 H. B. Mann and D. R. Whitney, *Ann. Math. Stat.*, 1947, **18**, 50–60, DOI: **10.1214/aoms/1177730491**.
59 J. Gu, B. Yang, M. Brauer and K. M. Zhang, *Atmos. Environ.*, 2021, **246**, 118125.
60 M. Lee, M. Brauer, P. Wong, R. Tang, T. H. Tsui, C. Choi, W. Cheng, P. C. Lai, L. Tian, T. Q. Thach, R. Allen and B. Barratt, *Sci. Total Environ.*, 2017, **592**, 306–315.
61 X. Ma, B. Zou, J. Deng, J. Gao, I. Longley, S. Xiao, B. Guo, Y. Wu, T. Xu, X. Xu, X. Yang, X. Wang, Z. Tan, Y. Wang, L. Morawska and J. Salmond, *Environ. Int.*, 2024, **183**, 108430.
62 M. Eeftens, R. Beelen, K. De Hoogh, T. Bellander, G. Cesaroni, M. Cirach, C. Declercq, A. Dedele, E. Dons, A. De Nazelle, K. Dimakopoulou, K. Eriksen, G. Falq, P. Fischer, C. Galassi, R. Gražulevičiene, J. Heinrich, B. Hoffmann, M. Jerrett, D. Keidel, M. Korek, T. Lanki, S. Lindley, C. Madsen, A. Mölter, G. Nádor, M. Nieuwenhuijsen, M. Nonnemacher, X. Pedeli, O. Raaschou-Nielsen, E. Patelarou, U. Quass, A. Ranzi, C. Schindler, M. Stempfelet, E. Stephanou, D. Sugiri, M. Y. Tsai, T. Yli-Tuomi, M. J. Varró, D. Vienneau, S. Von Klot, K. Wolf, B. Brunekreef and G. Hoek, *Environ. Sci. Technol.*, 2012, **46**, 11195–11205.
63 M. Eeftens, R. Meier, C. Schindler, I. Aguilera, H. Phuleria, A. Ineichen, M. Davey, R. Ducret-Stich, D. Keidel, N. Probst-Hensch, N. Künzli and M. Y. Tsai, *Environ. Health: Global Access Sci. Source*, 2016, **15**, 1–14.
64 G. Hoek, R. Beelen, G. Kos, M. Dijkema, S. C. V. Der Zee, P. H. Fischer and B. Brunekreef, *Environ. Sci. Technol.*, 2011, **45**, 622–628.

65 S. Vardoulakis, B. E. A. Fisher, K. Pericleous and N. Gonzalez-Flesca, *Atmos. Environ.*, 2003, **37**, 155–182.
66 L. J. Hunter, G. T. Johnson and I. D. Watson, *Atmos. Environ. Part B, Urban Atmos.*, 1992, **26**, 425–432.
67 Z. Wu, X. Zhang and M. Wu, *J. Cleaner Prod.*, 2016, **112**, 1658–1666.
68 C. Lin, M. Hsie, W. Hsiao, H. Wu and T. Cheng, *J. Perform. Constr. Facil.*, 2012, **26**, 203–211.
69 G. P. Compo, Research Data Archive at the National Center for Atmospheric Research, Computational and Information Systems Laboratory, DOI: **10.5065/D6SQ8XDW**, accessed 2 May 2022.